ISSN 0006-2979, Biochemistry (Moscow), 2025, Vol. 90, No. 12, pp. 1775-1788 © Pleiades Publishing, Ltd., 2025.
Russian Text © The Author(s), 2025, published in Biokhimiya, 2025, Vol. 90, No. 12, pp. 1902-1916.

REVIEW

Microbial 2-Enoate Reductases Containing Covalently Bound Flavin Mononucleotide

Alexander V. Bogachev[1,a]*, Alexander A. Baykov[1], Victor A. Anashkin[1], and Yulia V. Bertsova[1]

[1]*Belozersky Institute of Physico-Chemical Biology, Lomonosov Moscow State University, 119234 Moscow, Russia*
[a]*e-mail: bogachev@belozersky.msu.ru*

Received June 20, 2025
Revised August 10, 2025
Accepted August 11, 2025

Abstract—Flavin mononucleotide (FMN) and flavin adenine dinucleotide (FAD) are prosthetic groups of many enzymes and can be attached to proteins either covalently or non-covalently. Covalent attachment of FMN to Thr or Ser residues via a phosphate group is catalyzed by the recently discovered enzyme flavin transferase. Among the enzymes containing phosphoester-linked FMN, the most widely represented ones are various microbial 2-enoate reductases catalyzing reduction of unsaturated carboxylic acids (fumaric, acrylic, cinnamic, urocanic, etc.). The review is focused on microbial 2-enoate reductases and discusses their classification by domain organization and intracellular location, structural basis of substrate specificity, catalytic mechanism, and function, as well as the significance and evolutionary origin of the covalent attachment of FMN as a prosthetic group.

DOI: 10.1134/S0006297925601819

Keywords: anaerobic respiration, detoxification of 2-enoates, covalently bound FMN, catalytic mechanism

INTRODUCTION

Flavin adenine dinucleotide (FAD) and flavin mononucleotide (FMN) are the most typical prosthetic groups of proteins. Flavoproteins make up to 3.5% of the cellular proteome [1] and usually catalyze various redox reactions [2]. Most often, flavins are bound noncovalently, but in ~10% flavoproteins, they are linked to the protein by a covalent bond. In most cases, this bond is formed between the C8α or C6 atoms of the flavin isoalloxazine ring and His, Tyr, or Cys residues of the protein [3]. It is believed that the attachment through the isoalloxazine ring is autocatalytic but can be accelerated by a specific chaperone [4, 5].

FMN can also be attached to Thr and Ser residues via a phosphoester bond with the formation of a phosphodiester (Fig. 1) [6]. As has been shown for the first time for the Na^+-translocating NADH:quinone oxidoreductase of the bacterial respiratory chain, such posttranslational modification is performed by a special enzyme, flavin transferase ApbE, which uses FAD as a substrate [7]. ApbE recognizes the consensus DgxtsA**T**/**S** motif (modified Thr or Ser residues are shown in bold) in the target protein [7-10].

The gene for flavin transferase has been identified only in some eukaryotic genomes; it is moderately common among archaea and widespread among bacteria [7] (is present in a half of bacterial genomes [11]). Interestingly, ApbE is found in prokaryotes much more frequently than the Na^+-translocating NADH:quinone oxidoreductase, which is an indirect evidence of flavinylation by ApbE of other bacterial proteins [7, 12].

In general, proteins flavinylated by ApbE have been studied much less compared to proteins in which flavin is bound through the isoalloxazine ring (covalently or noncovalently). Microbial 2-enolate reductases are examples of enzymes containing FMN residues linked via a phosphoester bond. They catalyze reduction of 2-enoate with the formation of an anion of the respective saturated carboxylic acid (1):

$$R–CH=CH–COO^- \xrightarrow{2H} R–CH_2–CH_2–COO^-. \quad (1)$$

* To whom correspondence should be addressed.

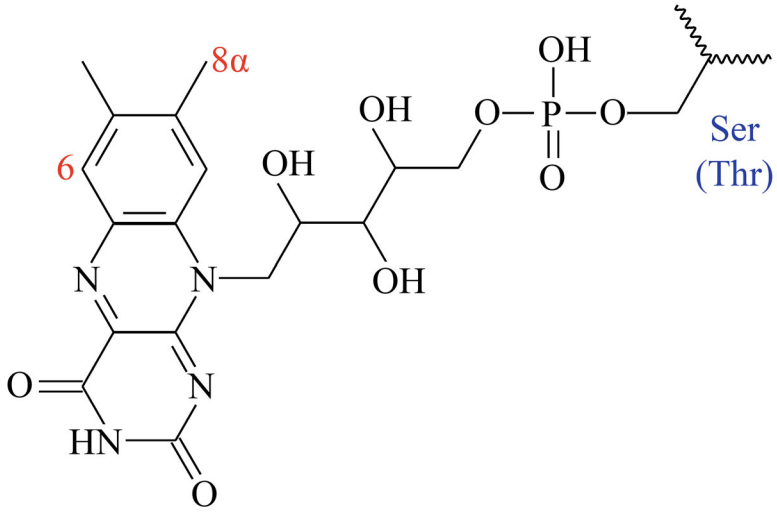

Fig. 1. FMN covalent attachment via a phosphate group to Ser (Thr) protein residues. C6 and C8α atoms of the isoalloxazine ring (shown in red) can form N–C, O–C or S–C bonds with His, Tyr, or Cys residues, respectively (not discussed in the review).

2-Enoates (anions of fumaric, acrylic, cinnamic, urocanic, and other acids) are widely represented in cells; the specificity of 2-enoate reductases is determined by the nature of the R substituent. In this review, we discuss classification of 2-enoate reductases according to the domain organization and intracellular location, the structural bases of their substrate specificity, the catalytic mechanism, and function of these enzymes, as well as the significance and evolutionary origin of the covalent attachment of FMN as a prosthetic group.

DOMAIN STRUCTURE OF MICROBIAL 2-ENOATE REDUCTASES

In prokaryotic genomes, the genes of functionally related proteins are often grouped together [13, 14], so that the functional relationship of these proteins can be predicted by the analysis of the genomic context [15]. In particular, genomic analysis has shown that the *apbE* gene and genes of proteins containing the *FAD_binding_2* domain (Pfam ID: PF00890) are frequently located close to each other [11]. Moreover, these proteins usually contain either the *FMN_bind* domain (PF04205 [16, 17]) flavinylated by ApbE or an amino acid sequence that includes the potential flavinylation motif DgxtsAT/S (although not recognized as an individual domain by bioinformatics algorithms) (Fig. 2).

The *FAD_binding_2* domain is widespread among eukaryotes and prokaryotes; it is a component of succinate dehydrogenase (complex II of the respiratory chain), fumarate reductase, aspartate oxidase, glutathione reductase, and some other enzymes [18, 19]. This domain contains FAD (most often, noncovalently bound) and catalytic sites for substrate oxidation/reduction. In most cases, the *FAD_binding_2* domain

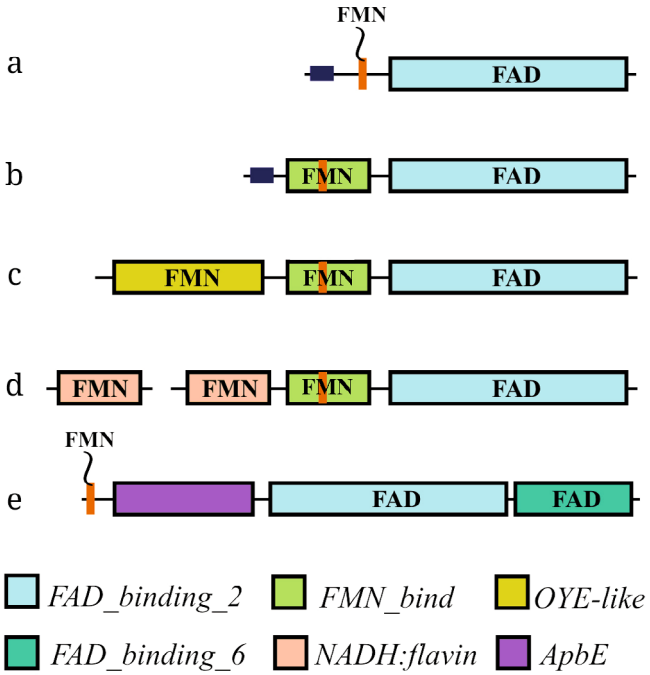

Fig. 2. a-e) Domain architecture of microbial 2-enoate reductases containing covalently bound FMN (according to the InterPro database [63]). The *FAD_binding_2* (PF00890), *FMN_bind* (PF04205), *OYE-like* (PF00724), *FAD_binding_6* (PF00970), *NADH:flavin* (PF03358) and *ApbE* (PF02424) domains are indicated by different colors; redox-active prosthetic groups of the domains are given within rectangles; signal peptides are shown as small dark blue rectangles; flavinylation motif DgxtsAT/S is shown in red (see the text for the examples of experimentally studied proteins with the indicated types of domain architecture).

reduces 2-enoate with the formation of respective carboxylic acid or performs the reverse reaction, i.e., oxidation of carboxylic acid with the formation of respective 2-enoate. The most typical substrate of 2-enoate reductases is fumarate. It is typically reduced by the membrane-bound quinol:fumarate oxidoreductase complex, which contains the *FAD_binding_2* domain and is structurally similar to complex II of the respiratory chain [20]. Only some microorganisms use periplasmic flavocytochromes *c* consisting of the *FAD_binding_2* domain and the heme C-containing cytochrome domain for anaerobic respiration; these domains may be parts of a single polypeptide or belong to two different subunits. The donor of reducing equivalents for flavocytochromes is usually low-potential cytochrome *c* [18, 19, 21].

The functioning of the *FAD_binding_2* domain is provided by the electron transfer from an external donor/acceptor (e.g., quinol or cytochrome *c*) to FAD. This electron transport pathway is usually formed by hemes or FeS clusters of accessory domains or subunits. In 2-enoate reductases shown in Fig. 2, the transfer of electrons from the external donor of reducing equivalents to the substrate most probably involves covalently bound FMN.

PERIPLASMIC (EXTRACELLULAR) FUMARATE REDUCTASES AND UROCANATE REDUCTASES OF THE ANAEROBIC RESPIRATORY CHAIN

The proteins shown in Fig. 2, a and b, contain the C-terminal domain *FAD_binding_2* and the N-terminal fragment or domain capable of attaching FMN through a phosphoester bond. The N-terminal sequences of these proteins also contain the Sec- or Tat-type signal peptides, suggesting periplasmic (extracellular) location of mature proteins. In most cases, these signal peptides include the site for the covalent attachment of lipids. Therefore, the corresponding proteins are lipoproteins linked to the outer surface of bacterial cytoplasmic membrane.

The proteins shown in Fig. 2a are common among anaerobic Gram-positive bacteria. In most cases, these proteins are extracellular fumarate reductases of the anaerobic respiratory chain, which are structurally similar to flavocytochromes *c* and differ from them only in that the electron transfer to the catalytic site in these enzymes involves covalently bound FMN instead of hemes C. This has been verified for the extracellular fumarate reductase FrdA (UniProt ID: Q8YA11) from the pathogenic bacterium *Listeria monocytogenes* [22]. Indeed, the strain of this bacterium with the disrupted *frdA* gene lost the ability for anaerobic growth with fumarate as the terminal electron acceptor. The functioning of FrdA requires its flavinylation and the presence of a system for the extracellular electron transfer, which seems to be the source of reducing equivalents for fumarate reduction in *L. monocytogenes* [22].

The substrate specificity of proteins containing the *FMN_bind* domain in the N-terminal region (Fig. 2b) is different. For example, the periplasmic (extracellular) urocanate reductase UrdA (Q8CVD0) from the bacterium *Shewanella oneidensis* MR-1 reduces urocanic acid at a high rate but is inactive toward fumaric or any other natural α,β-unsaturated carboxylic acid [23]. The functioning of this protein allows *S. oneidensis* to use urocanate as the terminal electron acceptor for anaerobic respiration [23]. A natural donor of reducing equivalents for this enzyme is membrane-bound noncoupled menaquinol:-cytochrome *c* oxidoreductase CymA [24]. Similar data were obtained for UrdA from *Enterococcus rivorum* [22]. Flavinylation of UrdA is necessary for its enzymatic activity and physiological function [22, 23].

The structures of full-length FrdA and UrdA, not determined experimentally, have been predicted with AlphaFold2 [25] or Chai-1 [26] (Fig. 3, a and b). According to the obtained model, the N-terminal region of FrdA (shown in black in Fig. 3a) followed by the *FAD_binding_2* domain is bound to the latter via a flexible linker and forms an α-helix adjacent to the main part of the enzyme. Notably, the covalently bound FMN is close to FAD (edge-to-edge distance, 5.4 Å), which should allow rapid electron transfer between the two flavins. In the model of UrdA, the covalently bound FMN of the *FMN_bind* domain is also located in close proximity to FAD of the *FAD_binding_2* domain (edge-to-edge distance, 7 Å) (Fig. 3b). The access to the FMN residue on the surface of the UrdA molecule is sterically hindered, which may prevent its reduction by external reducers, at least large-size ones, such as cytochrome *c*. Since the *FAD_binding_2* and *FMN_bind* domains in UrdA are linked to each other via a flexible linker (Fig. 3b), the latter domain can presumably shift away from the *FAD_binding_2* domain to accept electrons from cytochrome *c*. Therefore, we assume that the covalently bound FMN in FrdA and UrdA acts as a mobile electron carrier transporting electrons from an external source of reducing equivalents to FAD of the catalytic domain.

CYTOPLASMIC NADH:2-ENOATE REDUCTASES OF BACTERIA

Potential flavinylated 2-enoate reductases with a more complex domain architecture (Fig. 2, c and d) contain the C-terminal *FAD_binding_2* catalytic domain and the *FMN_bind* domain with the covalently bound FMN, which make them similar to the

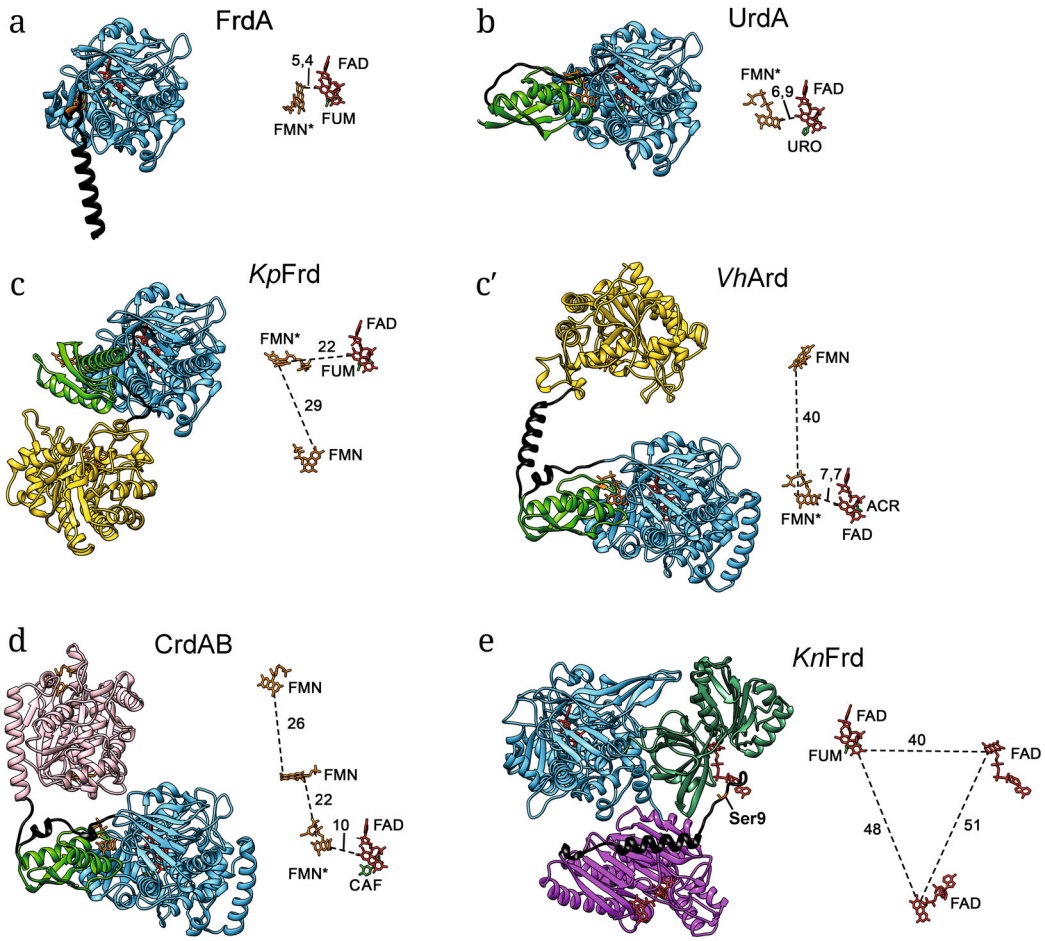

Fig. 3. The structures of full-length 2-enoate reductases containing covalently bound FMN: a) fumarate reductase FrdA from *L. monocytogenes*; b) urocanate reductase UrdA from *S. oneidensis*; c) NADH:fumarate reductase *Kp*Frd from *Klebsiella pneumoniae*; c′) NADH:acrylate reductase *Vh*Ard from *Vibrio harveyi*; d) NADH:hydroxycinnamate reductase CrdAB from *Vibrio ruber*; e) NADH:fumarate reductase *Kn*Frd from *Leptomonas pyrrhocoris*. Domains and linkers are colored as in Fig. 2. The structures were predicted with AlphaFold 2.3.2; FAD was positioned in the *FAD_binding_2*, *ApbE*, and *FAD_binding_6* domains like in crystal structures (PDB codes: 1D4E, 3PND, and 2EIX, respectively); FMN was covalently bound to the *FMN_bind* domain like in the 4XA7 structure, noncovalently bound to for the *OYE-like* domain like in the 5DXY structure, or docked to the *NADH:flavin* domains with AutoDock Vina 1.2.5 [64]. The structure of FrdA with FMN (covalently bound to Ser27) and FAD (panel a) was obtained with Chai-1 [26]. Fumarate (FUM) and urocanate (URO) substrates were transferred from the 1D4E and 6T87 structures; acrylate (ACR) and caffeate (CAF) were docked using AutoDock Vina. Positions of redox-active cofactors and substrates are shown to the right of each model; the distances between them are given in Å; red, FAD; orange, FMN (covalently bound FMN is designated as FMN*); green, substrate. All images are shown to the same scale.

above-described urocanate reductases of anaerobic respiratory chain. However, they lack the signal peptides and, therefore, have to be located in the cytoplasm. In addition, they include either *OYE* (old yellow enzyme)-like (PF00724) or *NADH:flavin* (PF03358) accessory N-terminal domains that typically contain a noncovalently bound FMN and are able to oxidize NAD(P)H. Hence, proteins shown in Fig. 2, c and d are putative cytoplasmic NAD(P)H:2-enoate reductases.

The *OYE-like* domain was found in the NADH:fumarate reductase *Kp*Frd (B5XRB0) from the enteric bacterium *Klebsiella pneumoniae* [27, 28] and in the cytoplasmic NADH:acrylate reductase *Vh*Ard (P0DW92) from the marine bacterium *Vibrio harveyi* [29] (Fig. 2c). The molecule of *Kp*Frd contains three flavins (noncovalently bound FAD and FMN and covalently bound FMN) as prosthetic groups [27]. This protein reduces fumarate at high rates (~500 turnovers per sec) when using the artificial electron donor methyl viologen. Among natural donors of reducing equivalents, *Kp*Frd oxidizes only NADH, which allows it to catalyze the NADH:fumarate reductase reaction at a rate of ~10 turnovers per sec under anaerobic conditions [28].

The model of 3D structure of *Kp*Frd obtained with AlphaFold2 is shown in Fig. 3c. The distances between the flavins in this protein are too large to maintain a physiologically significant rate of electron transfer.

Therefore, during the catalytic cycle of *Kp*Frd, its domains likely undergo conformational rearrangements, which consequentially reduces the distances between different pairs of the flavin prosthetic groups. The *FMN_bind* domain is bound to the *FAD_binding_2* and *OYE-like* domains via flexible linkers, thus allowing the covalently bound FMN to move between FAD of the *FAD_binding_2* domain and FMN of the *OYE-like* domain. Hence, the covalently bound FMN functions as a mobile carrier of electrons between different domains of *Kp*Frd.

Measuring the kinetics of *Kp*Frd reduction in the presence of NADH has made it possible to elucidate the mechanism of electron transfer in this protein [28]. NADH oxidation in the *OYE-like* domain results in the reduction of noncovalently bound FMN. Next, the electrons are transferred to the covalently bound FMN in the *FMN_bind* domain and then to noncovalently bound FAD and fumarate. The slowest step, which limits the rate of enzyme turnover, is the transfer of electrons between noncovalently and covalently bound FMN entities.

The *Vh*Ard protein encoded in the genome of *V. harveyi* has identical domain architecture. It contains the same prosthetic groups and is able to oxidize NADH [29]. However, the spatial location of its domains in the predicted 3D structure is different from that in *Kp*Frd. In *Vh*Ard, the *FAD_binding_2* and *FMN_bind* domains are closer to each other (Fig. 3c′); hence, the distance between FAD and covalently bound FMN is reduced to 7.7 Å, while the distance between two FMN molecules is increased to 40 Å. This observation confirms the above assumption that the covalently bound FMN in the *FMN_bind* domain can act as a mobile carrier of electrons between different protein domains. The structures of *Kp*Frd and *Vh*Ard might represent the two implemented variants of mutual location of the domains.

The screening of natural α,β-unsaturated carboxylic acids has shown that *Vh*Ard readily reduces acrylic and methacrylic acids, but not fumaric and other unsaturated carboxylic acids. The catalytic efficiency of *Vh*Ard toward acrylate proved to be 330 times higher than toward methacrylate; hence, this enzyme could be identified as NADH:acrylate reductase [29].

Cytoplasmic NADH:(hydroxy)cinnamate reductase CrdAB (A0A1R4LHH9 and A0A1R4LHW6) from the marine bacterium *Vibrio ruber* is a characterized representative of flavoproteins with the structure shown in Fig. 2d. This protein contains four flavin cofactors (noncovalently bound FAD and two FMNs and covalently bound FMN) as prosthetic groups. The substrate specificity of CrdAB is unique, as it reduces only (hydroxy)cinnamic acids: (cinnamic, ferulic, *p*-coumaric, and caffeic) among natural 2-enoates [30]. Although CrdAB is structurally similar to the enzymes described above, the domain responsible for NADH oxidation in this protein is the N-terminal *NADH:flavin* domain.

An interesting property of Crd is that the genome of *V. ruber* contains the *crdA* gene (Fig. 2d), encoding a protein homologous to the *NADH:flavin* domain of CrdB (51% identity), upstream of the *crdB* gene. Prokaryotic NADH:flavin reductases are typically encoded by a single gene; however, they function as homodimers that noncovalently bind two FMN molecules (prosthetic groups) in the area of contact between the monomers [31, 32]. The homodimeric structure of NADH:flavin reductase seems to hinder the fusion of this protein with other proteins with the formation of an extended multidomain polypeptide. It is possible that the original NADH:flavin reductase gene had undergone duplication prior to the domain fusion during the evolution of CrdB. Next, one of the two resultant genes fused with the precursor of the *crdB* gene, while the second one remained a separate gene encoding an additional Crd subunit (CrdA).

Modeling the 3D structure of CrdAB [30] showed that this protein consists of two parts connected with a flexible linker (Fig. 3d). One part includes the *FAD_binding_2* and *FMN_bind* domains and is structurally similar to UrdA (Fig. 3b). The second part consists of the CrdA subunit and homologous N-terminal *NADH:flavin* domain of the CrdB subunit. Such structure is similar to the 3D structures of homodimeric NADH:flavin reductases [31, 32]. The edge-to-edge distance between FAD and covalently bound FMN is ~10 Å (Fig. 3d), which should allow rapid electron transfer between these flavin groups. Contrary to the above, the distance between the covalently bound FMN and the closest noncovalently bound FMN is ~22 Å (Fig. 3), which should prevent electron transfer between them at a rate sufficient for the catalysis of the NADH:cinnamate reductase reaction. Therefore, to ensure electron transfer between noncovalently and covalently bound FMN molecules during its catalytic cycle, Crd must adopt an alternative conformation that brings these two flavin groups closer to each other.

NADH:FUMARATE REDUCTASES OF KINETOPLASTIDS

In eukaryotic genomes, the *apbE* gene of flavin transferase has been found only in some protists, first of all, kinetoplastids. These parasitic microorganisms contain glycosomal and mitochondrial forms of NADH:fumarate reductase (*Kn*Frd) functioning in the matrix of the respective organelles and allowing anaerobic respiration in the gut of a carrier insect [33-35]. *Kn*Frd is important for the development

of the parasite procyclic form; therefore, it is considered as one of the potential targets for treating (preventing) various diseases caused by *Trypanosoma* and *Leishmania* species [36, 37]. The molecule of *Kn*Frd contains the *FAD_binding_2* domain for fumarate reduction and the *FAD_binding_6* (PF00970) domain for NADH oxidation. *Kn*Frd also includes an additional N-terminal domain homologous to the prokaryotic flavin transferase ApbE (Fig. 2e) [35]. *Kn*Frd produced in *Saccharomyces cerevisiae* [38] or *Trypanosoma brucei* [39] cells contained at its N-terminus covalently bound FMN attached to a conserved Ser residue. Usually, flavinylation of proteins by FMN is catalyzed by ApbE protein. However, in the case of *Kn*Frd, flavinylation occurs due to the activity of the intrinsic *ApbE* domain. The *ApbE* domain can covalently attach FMN residue both to the same molecule (*cis*-flavinylation) and to other *Kn*Frd molecules (*trans*-flavinylation), *cis*-flavinylation being more efficient than *trans*-flavinylation [39].

The model of the *Kn*Frd 3D structure is shown in Fig. 3e. In this enzyme, the distance (40 Å) between the NADH dehydrogenase site (FAD in the *FAD_binding_6* domain) and fumarate reductase site (FAD in the *FAD_binding_2* domain) is too long (40 Å) for direct electron transfer between them. The substitution of flavinylated Ser residue in the *Kn*Frd sequence deprives the mutant protein of covalently bound flavin and, as a consequence, leads to the complete loss of the NADH:fumarate reductase activity [38]. Apparently, the functional role of FMN in this protein is the transfer of reducing equivalents from the NADH dehydrogenase site (*FAD_binding_6* domain) to its fumarate reductase site (*FAD_binding_2* domain). Despite the fact that the site of FMN covalent attachment in *Kn*Frd has been established, the site of noncovalent binding of the isoalloxazine ring of this prosthetic group remains unknown. One can note a very short length of *Kn*Frd regions that cannot be assigned to the conserved *ApbE*, *FAD_binding_2*, and *FAD_binding_6* domains, as well as the low level of conservation of amino acid residues in these regions [38]. Hence, the primary structure of Frd has no regions capable of forming one more flavin-binding domain. This is in agreement with the idea that the covalently bound FMN located at the flexible N-terminal linker can be alternately found close to the FAD molecules in the *FAD_binding_6* and *FAD_binding_2* domains, acting as a mobile electron carrier between these domains.

THE ROLE OF COVALENTLY BOUND FMN IN 2-ENOATE REDUCTASES

In 2-enoate reductases of the anaerobic respiratory chain (Fig. 2, a and b), covalently bound FMN forms the pathway for the electron transport from the external donor of reducing equivalents to the catalytic 2-enoate reductase site and is a functional analog of C-type hemes in flavocytochromes *c* [18, 19, 21]. Iron contained in the heme is the most widespread transition metal in the Earth's crust. Hence, it is not surprising that living organisms use Fe very extensively for the catalysis of redox and other reactions. For example, iron is a component of universal prosthetic groups such as hemes, FeS clusters, nonheme Fe centers, etc. However, the saturation of the Earth's atmosphere with oxygen due to the appearance and development of oxygenic photosynthesis has caused large-scale oxidation of Fe^{2+} to Fe^{3+}. The low solubility of $Fe(OH)_3$ at neutral and especially alkaline pH values has led to a significant decrease in the content of soluble iron in many ecological niches, i.e., to the decrease in the availability of iron for modern living organisms.

Living organisms use several approaches to overcome the shortage in soluble forms of iron. One of them is replacement of iron-containing enzymes by enzymes that lack iron but perform the same function. The classical example of such strategy is the substitution of the [Fe-S]-containing ferredoxin for flavin-containing flavodoxin in many bacteria and algae, when their growth is limited by a source of iron [40-42]. Replacement of hemes C in flavocytochromes *c* with covalently bound FMN might be another example [11].

Why was a covalently linked flavin chosen for this substitution? Most frequently, flavins are covalently attached to proteins through the formation of a chemical bond between the isoalloxazine ring of this prosthetic group and an amino acid residue. It is believed that the physiological implication of such modification is an increase in the redox potential of the flavin prosthetic group, which is necessary for the catalytic activity of the respective flavoproteins [3]. On the contrary, FMN attachment via a phosphoester bond occurs far from the isoalloxazine ring (Fig. 1), so that such modification unlikely leads to significant changes in the redox properties of flavin. On the other hand, in the overwhelming majority of bacterial proteins, the domains that covalently bind FMN via a phosphoester bond have a periplasmic (extracellular) location [8, 27]. All the above leads to the conclusion that the covalent attachment of FMN is necessary for preventing dilution of this cofactor by the external environment upon partial dissociation of its noncovalent complexes with periplasmic (extracellular) proteins. The covalent attachment of heme C in cytochromes *c* has been explained in a similar way [43], which once again emphasizes the functional analogy between these two prosthetic groups.

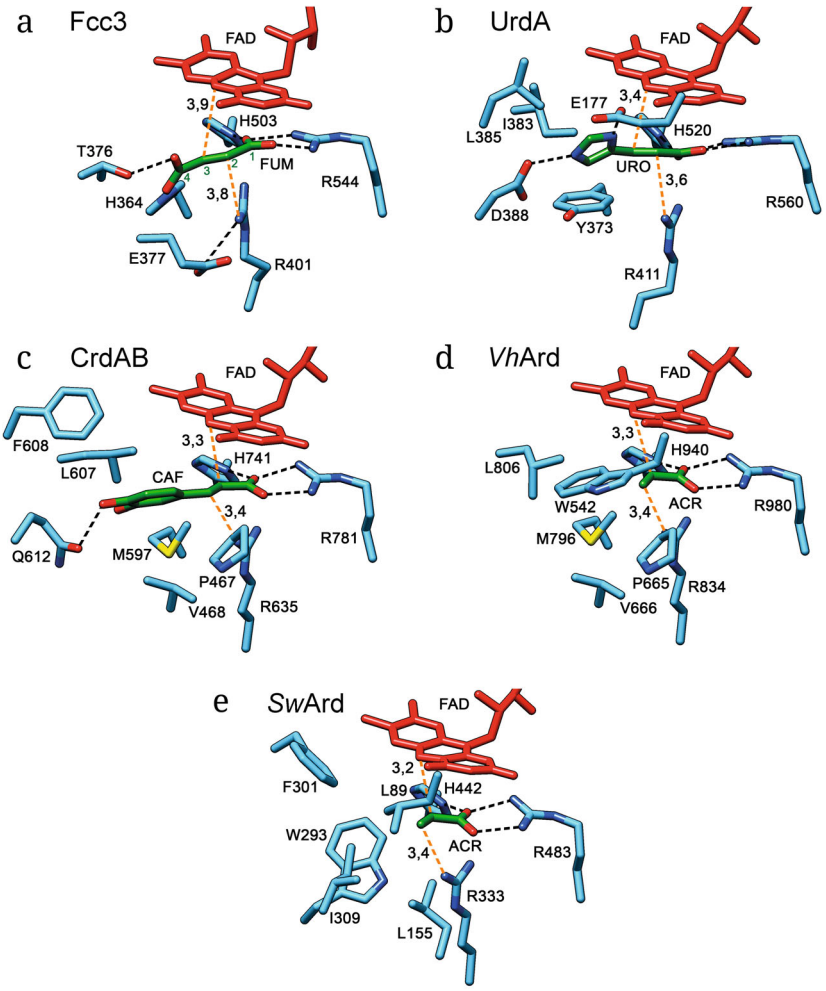

Fig. 4. Active sites of 2-enoate reductases with bound substrates. Structures a and b were obtained by X-ray crystallographic analysis; all other structures were predicted with AlphaFold (Fig. 3). a) Fumarate reductase Fcc_3 (PDB ID: 1D4E) with fumarate (FUM) [18]; b) urocanate reductase UrdA (PDB ID: 6T87) with urocanate (URO) [46]; c) hydroxycinnamate reductase CrdAB with caffeate (CAF); d and e) acrylate reductases *Vh*Ard and *Sw*Ard, respectively, with acrylate (ACR). Red, FAD; green, substrate (the numbering of the C-atoms of fumarate is indicated by green numbers); black dashed lines, hydrogen bonds; red dashed lines, distances (Å) between N5 atom of FAD and C3 atom of substrate and between N atom of Arg residue and C2 atom of substrate.

However, this explanation cannot be extended to intracellular NADH:2-enoate reductases (Fig. 2, c-e). In their cases, covalent binding of FMN via the phosphoester bond may result from the evolutionary origin of NADH:2-enoate reductases from extracellular reductases of the anaerobic respiratory chain (Fig. 2b). An alternative explanation is the following. FMN covalently linked via the phosphoester bond is similar to biotin and lipoic acid in that the functional part of all these prosthetic groups is attached to proteins via a long and flexible linker. Since biotin and lipoate act as mobile carriers of chemical groups during catalysis [44, 45], the covalent binding of FMN via a long and flexible linker may also contribute to its function as a mobile carrier (in this case, of reducing equivalents) between different domains of NADH:2-enoate reductases.

THE CATALYTIC MECHANISM AND SUBSTRATE SPECIFICITY OF 2-ENOATE REDUCTASES

Understanding the mechanisms of enzymatic catalysis is based primarily on the knowledge of spatial structures of the enzymes' active sites. For 2-enoate reductases, this information includes the structures of the catalytic fragments of flavocytochrome *c* (Fcc_3) (PDB IDs: 1D4E; 1Y0P) [18, 19] and UrdA (PDB ID: 6T87) [46] from bacteria of the *Shewanella* genus determined by X-ray analysis, predicted structures of the full-length enzymes (Fig. 3), and results of docking of prosthetic groups and substrates in the latter (Figs. 3 and 4). The validity of the structural prediction with the AlphaFold algorithm is supported by experimentally obtained structures of the enzymes.

In the crystal structure of Fcc_3 [18], fumarate is located in the catalytic site in a close proximity to FAD (Fig. 4a). Five amino acid residues interact with the carboxylic groups of fumarate: His364 and Thr376 with the C4 group; Arg544, Arg401, and His503 with the C1 group [18, 19]. The position of His364 is strictly conserved in all described fumarate reductases, including FrdA, *Kp*Frd, and *Kn*Frd (Fig. S1, Online Resource 1), so that the presence of His residue at this position makes it possible to predict the fumarate reductase activity in yet unstudied 2-enoate reductases.

The small distance (3.9 Å) between FAD and fumarate allows the transfer of hydride ion from the N5 atom of flavin to the C3 atom of the substrate. This transfer is accompanied by the proton transfer through the pathway formed by Arg380, Glu377, and Arg401 to the C2 atom of fumarate with the formation of succinate [18, 19]. Therefore, Arg401 not only participates in the binding of the C1 carboxylic group of the substrate, but also acts as a proton donor in the reduction of fumarate. In accordance with the above, the substitution of Arg401 for Lys resulted in a ~10,000-fold decrease in k_{cat} without any significant effect on K_m for fumarate [19]. The C4 carboxylic group of the bound fumarate in the active site of Fcc_3 is twisted and is out-of-plane of this compound. Such conformation, being an intermediate between the relaxed conformations of fumarate and succinate and, consequently, close to the transition state, apparently facilitates substrate reduction.

This catalytic mechanism presumably also operates in 2-enoate reductases with other substrate specificities. In urocanate reductase UrdA, urocanate binds in a close proximity to FAD (Fig. 4b) [46]. Like in fumarate reductases, the binding of the C1 carboxylic group of the substrate involves Arg and His residues (Arg560, Arg411, and His520 in UrdA from *S. oneidensis*) conserved in all 2-enoate reductases (Fig. S1, Online Resource 1). In addition, urocanate binds to the protein in the twisted conformation untypical of the free substrate. This is achieved due to the out-of-plane rotation of the urocanate imidazole ring caused by its interaction with the carboxylic groups of Asp388 and Glu177 residues. In line with the above, the substitution of Glu177 and especially Asp388 for Ala significantly reduced the catalytic activity of UrdA, but had no appreciable effect on the Michaelis constant for urocanate [47]. Like in fumarate reductases, Arg411 in UrdA acts as a proton donor in urocanate reduction, and its substitution leads to the complete loss of enzymatic activity [47]. The presence of negatively charged amino acids at positions corresponding to Asp388 and Glu177 of UrdA appears to be a characteristic feature of the primary structures of urocanate reductases, which distinguishes them from other 2-enoate reductases.

The 3D structures of active sites of other described 2-enoate reductases have not been determined experimentally, but they can be quite reliably modeled using AlphaFold (Fig. 3) followed by docking of the substrates to the active site (Fig. 4, c-e). The reliability of modeling is confirmed by the formation of a bond between the C1 carboxylic group of the substrate and conserved His and Arg residues (Fig. S1, Online Resource 1). In addition, the distances between the N5 atom of FAD and the C3 atom of the substrate, as well as between the N atom of conserved Arg residue and the C2 atom of the substrate (marked with red dashed lines in Fig. 4) in the models are similar to those determined experimentally, which provides rapid transfer of a hydride ion and a proton, respectively [18, 46].

The binding of the caffeate carboxylic group in the model of the CrdAB enzyme–substrate complex involves conserved Arg781, Arg635, and His741 residues. These interactions provide a sufficiently close positioning of caffeate relative to the N5 atom of FAD (3.7 Å) for the hydride ion transfer. The phenolic group of caffeate is located in a hydrophobic cavity formed by the Met597 and Leu607 residues and is out-of-plane of the substrate. The hydroxyl group of caffeate in the *para*-position is linked through a hydrogen bond to the Gln612 residue, which therefore can be considered as a determinant of specificity of 2-enoate reductases toward hydroxycinnamic acids. Interestingly, the *meta*-hydroxyl group of caffeate does not form contacts with the protein in the model of the CrdAB structure, which is in good agreement with the ability of CrdAB to reduce caffeic and *p*-coumaric acids with equal efficiencies [30].

The 3D model of the *Vh*Ard catalytic site also shows acrylate binding in a close proximity (3.8 Å) to FAD (Fig. 4d). This binding is achieved by the conserved 2-enoate reductase triad of Arg980, His940, and Arg834. The last residue also seems to be a proton donor in the acrylate reduction by the hydride ion. Acrylate binding takes place only through its carboxylic group; therefore, the specificity of *Vh*Ard is achieved due to the small size of the substrate-binding pocket formed by the large hydrophobic residues Pro665, Val666, Met796, and Leu806. However, these residues apparently do not determine the specificity of 2-enoate reductase for acrylate, because the size of the substrate-binding site can be reduced in different ways. In accordance with the above, the binding site of cytochrome *c*:acrylate reductase from *Shewanella woodyi* (*Sw*Ard) [48], which is similar in specificity to *Vh*Ard, is formed by other bulky hydrophobic residues (Fig. 4e; Fig. S1, Online Resource 1). What calls attention is the position of Trp542 in *Vh*Ard (Leu89 in *Sw*Ard); the occurrence of a bulky hydrophobic amino acid residue at this position might be

a determinant of 2-enoate reductase specificity for acrylate (Fig. 4, d and e; Fig. S1, Online Resource 1).

Analysis of bacterial genomes demonstrates a variability of amino acid residues of hypothetical 2-enoate reductases at positions responsible for the binding of fumarate, urocanate, acrylate, and hydroxycinnamates in the characterized homologous proteins. This fact suggests that the respective reductases are able to use some other compounds as terminal electron acceptors during anaerobic growth [22, 49].

THE PHYSIOLOGICAL ROLE OF 2-ENOATE REDUCTASES IN MICROORGANISMS

The main physiological role of the above-described extracellular (periplasmic) 2-enoate reductases is undoubtedly anaerobic respiration. Hence, inactivation of the *frdA* and *urdA* genes makes *L. monocytogenes* and *S. oneidensis* MR-1 cells incapable of anaerobic growth with fumarate and urocanate as terminal electron acceptors, respectively [22, 23]. Moreover, the synthesis of UrdA in *S. oneidensis* MR-1 cells is induced only under anaerobic conditions and only in the presence of urocanate in the growth medium [23], i.e., only under conditions when anaerobic respiration on urocanate is a beneficial process. Anaerobic respiration allows FrdA- and UrdA-containing bacteria to re-oxidize NADH formed during fermentation. Moreover, since the electron donor for UrdA is cytochrome *c* [24], the functioning of urocanate reductase allows for additional energy conservation in a form of transmembrane potential difference due to the functioning of the preceding component of the electron transport chain (complex I).

We should mention a potential significance of UrdA-like proteins for medicine. The products of bacterial anaerobic respiration can accumulate in the human intestine in large quantities and, as they are biologically active, affect the organism [50]. For example, Molinaro et al. [51] have shown that urocanate respiration is not characteristic of the microflora of healthy people but is observed in the gut of most patients with type 2 diabetes. Moreover, it has been established that imidazolyl propionate (the product of urocanate reduction by intestinal microflora) is absorbed into the blood and impairs glucose tolerance by suppressing intracellular signal transduction from insulin due to the inhibition of mTORC1 [52]. Therefore, the urocanate respiration of intestinal bacteria may be not the consequence but the direct cause of type 2 diabetes, which potentially suggests new approaches for treating this widespread disease.

The main role of intracellular NADH:fumarate reductases, such as *Kp*Frd of *K. pneumoniae* and *Kn*Frd of kinetoplastids, is also anaerobic respiration. For example, in kinetoplastids, succinate is one of the major fermentation products, while inactivation of the glycosomal and mitochondrial forms of *Kn*Frd completely prevents fumarate respiration [35]. The synthesis of *Kp*Frd in *K. pneumoniae* is induced only under anaerobic conditions in the presence of fumarate (malate) [28], which is also in good agreement with the involvement of this enzyme in anaerobic respiration. Under aerobic conditions, *Kp*Frd reduces O_2 both in the presence and absence of fumarate. The product of this reaction is hydrogen peroxide that can cause cell death. However, this activity might not be physiological, because the synthesis of *Kp*Frd is repressed under aerobic conditions [28].

The physiological role of intracellular NADH:fumarate reductases is still not quite clear. Why is it advantageous to use soluble NADH:fumarate reductase under certain conditions, if the same reaction can be performed with the involvement of membrane-bound enzymes of the respiratory chain (complex I and quinol:fumarate oxidoreductase) [53]? When the latter enzymes are active, the transfer of electrons from NADH to fumarate is accompanied not only by the NADH reoxidation but also by energy conservation in a form of transmembrane potential difference, which must be energetically more favorable compared to the functioning of noncoupled intracellular NADH:fumarate reductases. The use of *Kn*Frd in kinetoplastids can be accounted for by the inability of these microorganisms to synthesize a low-potential quinone (menaquinone or rhodoquinone) necessary for the membrane-associated fumarate respiration involving the electron transport chain [54]. However, *K. pneumoniae* cells can synthesize menaquinone [55], and the genome of this bacterium contains full set of genes encoding complex I and quinol:fumarate oxidoreductase. Therefore, it is possible that intracellular NADH:fumarate reductases perform some functions in addition to anaerobic respiration. Thus, it has been hypothesized that the generation of reactive oxygen species by *Kn*Frd of *T. brucei* in the absence of fumarate and in the presence of O_2 is required for the differentiation of the procyclic form of this parasite into epimastigotes [56].

On the contrary, the main physiological role of cytoplasmic NADH:acrylate reductase *Vh*Ard and NADH:(hydroxy)cinnamate reductase CrdAB is not anaerobic respiration but detoxification of acrylic and hydroxycinnamic acids. The synthesis of *Vh*Ard and CrdAB in bacterial cells is induced in the presence of acrylate and (hydroxy)cinnamates, respectively, regardless of oxygen concentration in the growth medium [29, 30]. Acrylate is an electrophilic compound capable of reacting with many cell components, which accounts for the toxic effect of acrylic acid [57, 58]. The major natural source of free acrylic

acid is dimethylsulfoniopropionate (DMSP) [59]. This compound is used as an osmolyte by many marine algae and accumulates in these organisms at very high concentrations. Decomposition of DMSP by microbial DMSP lyases results in the formation of acrylate [59], which makes acrylic acid quite typical for different marine ecological niches. The bacterium *V. harveyi* is often found in acrylate-rich niches (e.g., coral mucus) and can use this compound as the sole carbon and energy source [60]. *Vh*Ard-like proteins are also widespread among other representatives of marine bacteria of the genus *Vibrio* and apparently used to prevent the toxic effects of acrylic acid.

Similar function can be suggested for Crd-like NADH:(hydroxy)cinnamate reductases that reduce toxic hydroxy derivatives of cinnamic acid [61]. The most efficient substrates for CrdAB (caffeate and ferulate) are precursors in the synthesis of lignin and other phenolic secondary metabolites in terrestrial plants. Therefore, these compounds are widespread in various terrestrial habitats (e.g., soil and intestines of herbivores). Accordingly, Crd-like proteins are widespread among terrestrial anaerobic microorganisms, including bacteria of the human gut microbiome. These proteins are found in numerous representatives of the genera *Clostridium*, *Klebsiella*, *Citrobacter*, *Aeromonas*, *Paenibacillus*, *Streptococcus*, etc. In terrestrial bacteria, Crd-like proteins might be responsible for detoxification of hydroxycinnamic acids, but this hypothesis requires experimental verification. At the same time, reductases similar to CrdAB occur rarely in marine organisms. For example, the Blast search reveals Crd-like proteins only in marine bacteria of the *Vibrio* genus (*V. ruber*, *V. rhizosphaerae*, *V. gazogenes*, *V. salinus*, *V. spartinae*, and *V. tritonius*). The only known marine ecological niche enriched in hydroxycinnamic acids is the rhizosphere of marine angiosperms. It has been shown that these plants secrete caffeic acid to the rhizosphere, together with sucrose and various phenolic compounds [61]. It is noteworthy that the above-mentioned marine Crd-containing bacteria can be found only in the rhizosphere of marine angiosperms [62], so detoxification of caffeate by Crd-like proteins presumably allows Crd-containing marine bacteria to inhabit this sugar-rich ecological niche.

The use of the *NADH:flavin* domain instead of the *OYE-like* domain in Crd apparently gives this protein multiple advantages. A characteristic feature of NADH:2-enoate reductases is that under aerobic conditions, they spent a significant quantity of reducing equivalents not for the reduction of physiological electron acceptors, but for the reduction of O_2 with the production of reactive oxygen species [28]. For strictly anaerobic bacteria, such a feature of NADH:2-enoate reductases may be neutral. However, in the case of facultative anaerobes, this activity may lead to cell damage during transition to aerobic conditions. Notably, it has been shown that CrdAB, in contrast to other NADH:2-enoate reductases, is a regulated enzyme that can be converted into inactive form [30]. This inactivation is regulated by the stationary level of some reduced prosthetic group in CrdAB and involves the *NADH:flavin* domain. Such regulation allows to switch off the enzymatic activity of CrdAB at high O_2 concentrations to avoid the generation of reactive oxygen species. The inactivation is reversible and, when O_2 concentration decreases, reduced Crd is slowly converted into the active form.

In conclusion, 2-enoate reductases described in this review are widespread among anaerobic and facultative anaerobic microorganisms and perform functions such as anaerobic respiration, detoxification of 2-enoates, and cell cycle regulation by reactive oxygen species.

Abbreviations

ApbE	flavin transferase catalyzing covalent attachment of FMN to flavoproteins through a phosphoester bond
CrdAB	cytoplasmic NADH:(hydroxy)cinnamate reductase of *Vibrio ruber*
FAD	flavin adenine dinucleotide
Fcc_3	periplasmic fumarate reductase of bacteria of the *Shewanella* genus
FMN	flavin mononucleotide
FrdA	extracellular fumarate reductase of *Listeria monocytogenes*
*Kn*Frd	NADH:fumarate reductase of kinetoplastids
*Kp*Frd	cytoplasmic NADH:fumarate reductase of *Klebsiella pneumoniae*
OYE	old yellow enzyme
UrdA	bacterial periplasmic (extracellular) urocanate reductase
*Vh*Ard	cytoplasmic NADH:acrylate reductase of *Vibrio harveyi*

Supplementary information

The online version contains supplementary material available at https://doi.org/10.1134/S0006297925601819.

Acknowledgments

The work is dedicated to the memory of Vladimir Petrovich Skulachev.

Contributions

A.V.B. developed the study concept; A.A.B. and A.V.B. wrote the manuscript; V.A.A., analyzed 3D protein structures; Yu.V.B., V.A.A., and A.A.B. prepared the figures; A.V.B., A.A.B., V.A.A., and Yu.V.B. discussed and edited the manuscript.

Funding
The work was supported by the Russian Science Foundation (project no. 24-24-00043).

Ethics approval and consent to participate
This work does not contain any studies involving human or animal subjects.

Conflict of interest
The authors of this work declare that they have no conflicts of interest.

REFERENCES

1. Macheroux, P., Kappes, B., and Ealick, S. E. (2011) Flavogenomics – a genomic and structural view of flavin-dependent proteins, *FEBS J.*, **278**, 2625-2634, https://doi.org/10.1111/j.1742-4658.2011.08202.x.
2. Massey, V. (2000) The chemical and biological versatility of riboflavin, *Biochem. Soc. Trans.*, **28**, 283-296, https://doi.org/10.1042/0300-5127:0280283.
3. Heuts, D. P., Scrutton, N. S., McIntire, W. S., and Fraaije, M. W. (2009) What's in a covalent bond? On the role and formation of covalently bound flavin cofactors, *FEBS J.*, **276**, 3405-3427, https://doi.org/10.1111/j.1742-4658.2009.07053.x.
4. McNeil, M. B., and Fineran, P. C. (2013) Prokaryotic assembly factors for the attachment of flavin to complex II, *Biochim. Biophys. Acta*, **1827**, 637-647, https://doi.org/10.1016/j.bbabio.2012.09.003.
5. Maklashina, E., Iverson, T. M., and Cecchini, G. (2022) How an assembly factor enhances covalent FAD attachment to the flavoprotein subunit of complex II, *J. Biol. Chem.*, **298**, 102472, https://doi.org/10.1016/j.jbc.2022.102472.
6. Hayashi, M., Nakayama, Y., Yasui, M., Maeda, M., Furuishi, K., and Unemoto, T. (2001) FMN is covalently attached to a threonine residue in the NqrB and NqrC subunits of Na^+-translocating NADH-quinone reductase from *Vibrio alginolyticus*, *FEBS Lett.*, **488**, 5-8, https://doi.org/10.1016/s0014-5793(00)02404-2.
7. Bertsova, Y. V., Fadeeva, M. S., Kostyrko, V. A., Serebryakova, M. V., Baykov, A. A., and Bogachev, A. V. (2013) Alternative pyrimidine biosynthesis protein ApbE is a flavin transferase catalyzing covalent attachment of FMN to a threonine residue in bacterial flavoproteins, *J. Biol. Chem.*, **288**, 14276-14286, https://doi.org/10.1074/jbc.M113.455402.
8. Bogachev, A. V., Baykov, A. A., and Bertsova, Y. V. (2018) Flavin transferase: the maturation factor of flavin-containing oxidoreductases, *Biochem. Soc. Trans.*, **46**, 1161-1169, https://doi.org/10.1042/BST20180524.
9. Bertsova, Y. V., Serebryakova, M. V., Anashkin, V. A., Baykov, A. A., and Bogachev, A. V. (2019) Mutational analysis of the flavinylation and binding motifs in two protein targets of the flavin transferase ApbE, *FEMS Microbiol. Lett.*, **366**, fnz252, https://doi.org/10.1093/femsle/fnz252.
10. Fan, X., and Fraaije, M. W. (2025) Flavin transferase ApbE: from discovery to applications, *J. Biol. Chem.*, **26**, 108453, https://doi.org/10.1016/j.jbc.2025.108453.
11. Méheust, R., Huang, S., Rivera-Lugo, R., Banfield, J. F., and Light, S. H. (2021) Post-translational flavinylation is associated with diverse extracytosolic redox functionalities throughout bacterial life, *Elife*, **10**, e66878, https://doi.org/10.7554/eLife.66878.
12. Huang, S., Méheust, R., Barquera, B., and Light, S. H. (2024) Versatile roles of protein flavinylation in bacterial extracyotosolic electron transfer, *mSystems*, **9**, e0037524, https://doi.org/10.1128/msystems.00375-24.
13. Lawrence, J. (1999) Selfish operons: the evolutionary impact of gene clustering in prokaryotes and eukaryotes, *Curr. Opin. Genet. Dev.*, **9**, 642-648, https://doi.org/10.1016/s0959-437x(99)00025-8.
14. Koonin, E. V. (2011) *The Logic of Chance: The Nature and Origin of Biological Evolution*, Upper Saddle River, NJ, FT Press.
15. Rentzsch, R., and Orengo, C. A. (2009) Protein function prediction – the power of multiplicity, *Trends Biotechnol.*, **27**, 210-219, https://doi.org/10.1016/j.tibtech.2009.01.002.
16. Yeats, C., Bentley, S., and Bateman, A. (2003) New knowledge from old: *in silico* discovery of novel protein domains in *Streptomyces coelicolor*, *BMC Microbiol.*, **3**, 3, https://doi.org/10.1186/1471-2180-3-3.
17. Borshchevskiy, V., Round, E., Bertsova, Y., Polovinkin, V., Gushchin, I., Ishchenko, A., Kovalev, K., Mishin, A., Kachalova, G., Popov, A., Bogachev, A., and Gordeliy, V. (2015) Structural and functional investigation of flavin binding center of the NqrC subunit of sodium-translocating NADH:quinone oxidoreductase from *Vibrio harveyi*, *PLoS One*, **10**, e0118548, https://doi.org/10.1371/journal.pone.0118548.
18. Leys, D., Tsapin, A. S., Nealson, K. H., Meyer, T. E., Cusanovich, M. A., and Van Beeumen, J. J. (1999) Structure and mechanism of the flavocytochrome *c* fumarate reductase of *Shewanella putrefaciens* MR-1, *Nat. Struct. Biol.*, **6**, 1113-1117, https://doi.org/10.1038/70051.
19. Reid, G. A., Miles, C. S., Moysey, R. K., Pankhurst, K. L., and Chapman, S. K. (2000) Catalysis in fumarate reductase, *Biochim. Biophys. Acta*, **1459**, 310-315, https://doi.org/10.1016/s0005-2728(00)00166-3.
20. Cecchini, G., Schröder, I., Gunsalus, R. P., and Maklashina, E. (2002) Succinate dehydrogenase and fumarate reductase from *Escherichia coli*, *Biochim. Biophys. Acta*, **1553**, 140-157, https://doi.org/10.1016/s0005-2728(01)00238-9.
21. Arkhipova, O. V., and Akimenko, V. K. (2005) Unsaturated organic acids as terminal electron acceptors for reductase chains of anaerobic bacteria, *Microbiology*, **74**, 629-639, https://doi.org/10.1007/s11021-005-0116-6.

22. Light, S. H., Méheust, R., Ferrell, J. L., Cho, J., Deng, D., Agostoni, M., Iavarone, A. T., Banfield, J. F., D'Orazio, S. E. F., and Portnoy, D. A. (2019) Extracellular electron transfer powers flavinylated extracellular reductases in Gram-positive bacteria, *Proc. Natl. Acad. Sci. USA*, **116**, 26892-26899, https://doi.org/10.1073/pnas.1915678116.
23. Bogachev, A. V., Bertsova, Y. V., Bloch, D. A., and Verkhovsky, M. I. (2012) Urocanate reductase: identification of a novel anaerobic respiratory pathway in *Shewanella oneidensis* MR-1, *Mol. Microbiol.*, **86**, 1452-1463, https://doi.org/10.1111/mmi.12067.
24. Kees, E. D., Pendleton, A. R., Paquete, C. M., Arriola, M. B., Kane, A. L., Kotloski, N. J., Intile, P. J., and Gralnick, J. A. (2019) Secreted flavin cofactors for anaerobic respiration of fumarate and urocanate by *Shewanella oneidensis*: cost and role, *Appl. Environ. Microbiol.*, **85**, e00852-19, https://doi.org/10.1128/AEM.00852-19.
25. Jumper, J., Evans, R., Pritzel, A., Green, T., Figurnov, M., Ronneberger, O., Tunyasuvunakool, K., Bates, R., Žídek, A., Potapenko, A., Bridgland, A., Meyer, C., Kohl, S. A. A., Ballard, A. J., Cowie, A., Romera-Paredes, B., Nikolov, S., Jain, R., Adler, J., Back, T., Petersen, S., Reiman, D., Clancy, E., Zielinski, M., Steinegger, M., Pacholska, M., Berghammer, T., Bodenstein, S., Silver, D., Vinyals, O., Senior, A. W., Kavukcuoglu, K., Kohli, P., and Hassabis, D. (2021) Highly accurate protein structure prediction with AlphaFold, *Nature*, **596**, 583-589, https://doi.org/10.1038/s41586-021-03819-2.
26. Boitreaud, J., Dent, J., McPartlon, M., Meier, J., Reis, V., Rogozhnikov, A., and Wu, K. (2024) Chai-1: Decoding the molecular interactions of life, *bioRxiv*, https://doi.org/10.1101/2024.10.10.615955.
27. Bertsova, Y. V., Kostyrko, V. A., Baykov, A. A., and Bogachev, A. V. (2014) Localization-controlled specificity of FAD:threonine flavin transferases in *Klebsiella pneumoniae* and its implications for the mechanism of Na^+-translocating NADH:quinone oxidoreductase, *Biochim. Biophys. Acta*, **1837**, 1122-1129, https://doi.org/10.1016/j.bbabio.2013.12.006.
28. Bertsova, Y. V., Oleynikov, I. P., and Bogachev, A. V. (2020) A new water-soluble bacterial NADH: fumarate oxidoreductase, *FEMS Microbiol. Lett.*, **367**, fnaa175, https://doi.org/10.1093/femsle/fnaa175.
29. Bertsova, Y. V., Serebryakova, M. V., Baykov, A. A., and Bogachev, A. V. (2022) A novel, NADH-dependent acrylate reductase in *Vibrio harveyi*, *Appl. Environ. Microbiol.*, **88**, e0051922, https://doi.org/10.1128/aem.00519-22.
30. Bertsova, Y. V., Serebryakova, M. V., Anashkin, V. A., Baykov, A. A., and Bogachev, A. V. (2024) A redox-regulated, heterodimeric NADH:cinnamate reductase in *Vibrio ruber*, *Biochemistry (Moscow)*, **89**, 241-256, https://doi.org/10.1134/S0006297924020056.
31. Koike, H., Sasaki, H., Kobori, T., Zenno, S., Saigo, K., Murphy, M. E., Adman, E. T., and Tanokura, M. (1998) 1.8 Å crystal structure of the major NAD(P)H:FMN oxidoreductase of a bioluminescent bacterium, *Vibrio fischeri*: overall structure, cofactor and substrate-analog binding, and comparison with related flavoproteins, *J. Mol. Biol.*, **280**, 259-273, https://doi.org/10.1006/jmbi.1998.1871.
32. Agarwal, R., Bonanno, J. B., Burley, S. K., and Swaminathan, S. (2006) Structure determination of an FMN reductase from *Pseudomonas aeruginosa* PA01 using sulfur anomalous signal, *Acta Crystallogr. D Biol. Crystallogr.*, **62**, 383-391, https://doi.org/10.1107/S0907444906001600.
33. Mracek, J., Snyder, S. J., Chavez, U. B., and Turrens, J. F. (1991) A soluble fumarate reductase in *Trypanosoma brucei* procyclic trypomastigotes, *J. Protozool.*, **38**, 554-558, https://doi.org/10.1111/j.1550-7408.1991.tb06079.x.
34. Besteiro, S., Biran, M., Biteau, N., Coustou, V., Baltz, T., Canioni, P., and Bringaud, F. (2002) Succinate secreted by *Trypanosoma brucei* is produced by a novel and unique glycosomal enzyme, NADH-dependent fumarate reductase, *J. Biol. Chem.*, **277**, 38001-38012, https://doi.org/10.1074/jbc.M201759200.
35. Coustou, V., Besteiro, S., Rivière, L., Biran, M., Biteau, N., Franconi, J. M., Boshart, M., Baltz, T., and Bringaud, F. (2005) A mitochondrial NADH-dependent fumarate reductase involved in the production of succinate excreted by procyclic *Trypanosoma brucei*, *J. Biol. Chem.*, **280**, 16559-16570, https://doi.org/10.1074/jbc.M500343200.
36. Turrens, J. F., Newton, C. L., Zhong, L., Hernandez, F. R., Whitfield, J., and Docampo, R. (1999) Mercaptopyridine-N-oxide, an NADH-fumarate reductase inhibitor, blocks *Trypanosoma cruzi* growth in culture and in infected myoblasts, *FEMS Microbiol. Lett.*, **175**, 217-221, https://doi.org/10.1111/j.1574-6968.1999.tb13623.x.
37. Rodríguez Arce, E., Mosquillo, M. F., Pérez-Díaz, L., Echeverría, G. A., Piro, O. E., Merlino, A., Coitiño, E. L., Maríngolo Ribeiro, C., Leite, C. Q., Pavan, F. R., Otero, L., and Gambino, D. (2015) Aromatic amine N-oxide organometallic compounds: searching for prospective agents against infectious diseases, *Dalton Trans.*, **44**, 14453-14464, https://doi.org/10.1039/c5dt00557d.
38. Serebryakova, M. V., Bertsova, Y. V., Sokolov, S. S., Kolesnikov, A. A., Baykov, A. A., and Bogachev, A. V. (2018) Catalytically important flavin linked through a phosphoester bond in a eukaryotic fumarate reductase, *Biochimie*, **149**, 34-40, https://doi.org/10.1016/j.biochi.2018.03.013.
39. Schenk, R., Bachmaier, S., Bringaud, F., and Boshart, M. (2021) Efficient flavinylation of glycosomal fumarate reductase by its own ApbE domain in *Trypanosoma*

brucei, *FEBS J.*, **288**, 5430-5445, https://doi.org/10.1111/febs.15812.

40. Sancho, J. (2006) Flavodoxins: sequence, folding, binding, function and beyond, *Cell Mol. Life Sci.*, **63**, 855-864, https://doi.org/10.1007/s00018-005-5514-4.
41. LaRoche, J., Boyd, P. W., McKay, R. M. L., and Geider, R. J. (1996) Flavodoxin as an *in situ* marker for iron stress in phytoplankton, *Nature*, **382**, 802-805, https://doi.org/10.1038/382802a0.
42. Bertsova, Y. V., Kulik, L. V., Mamedov, M. D., Baykov, A. A., and Bogachev, A. V. (2019) Flavodoxin with an air-stable flavin semiquinone in a green sulfur bacterium, *Photosynth. Res.*, **142**, 127-136, https://doi.org/10.1007/s11120-019-00658-1.
43. Wood, P. M. (1983) Why do *c*-type cytochromes exist? *FEBS Lett.*, **164**, 223-226, https://doi.org/10.1016/0014-5793(83)80289-0.
44. Attwood, P. V. (1995) The structure and the mechanism of action of pyruvate carboxylase, *Int. J. Biochem. Cell Biol.*, **27**, 231-249, https://doi.org/10.1016/1357-2725(94)00087-r.
45. Douce, R., Bourguignon, J., Neuburger, M., and Rébeillé, F. (2001) The glycine decarboxylase system: a fascinating complex, *Trends Plant Sci.*, **6**, 167-176, https://doi.org/10.1016/s1360-1385(01)01892-1.
46. Venskutonytė, R., Koh, A., Stenström, O., Khan, M. T., Lundqvist, A., Akke, M., Bäckhed, F., and Lindkvist-Petersson, K. (2021) Structural characterization of the microbial enzyme urocanate reductase mediating imidazole propionate production, *Nat. Commun.*, **12**, 1347, https://doi.org/10.1038/s41467-021-21548-y.
47. Delavari, N., Zhang, Z., and Stull, F. (2024) Rapid reaction studies on the chemistry of flavin oxidation in urocanate reductase, *J. Biol. Chem.*, **300**, 105689, https://doi.org/10.1016/j.jbc.2024.105689.
48. Bertsova, Y. V., Serebryakova, M. V., Bogachev, V. A., Baykov, A. A., and Bogachev, A. V. (2024) Acrylate reductase of an anaerobic electron transport chain of the marine bacterium *Shewanella woodyi*, *Biochemistry (Moscow)*, **89**, 701-710, https://doi.org/10.1134/S0006297924040096.
49. Little, A. S., Younker, I. T., Schechter, M. S., Bernardino, P. N., Méheust, R., Stemczynski, J., Scorza, K., Mullowney, M. W., Sharan, D., Waligurski, E., Smith, R., Ramaswamy, R., Leiter, W., Moran, D., McMillin, M., Odenwald, M. A., Iavarone, A. T., Sidebottom, A. M., Sundararajan, A., Pamer, E. G., Eren, A. M., and Light, S. H. (2024) Dietary- and host-derived metabolites are used by diverse gut bacteria for anaerobic respiration, *Nat. Microbiol.*, **9**, 55-69, https://doi.org/10.1038/s41564-023-01560-2.
50. Koh, A., and Bäckhed, F. (2020) From association to causality: the role of the gut microbiota and its functional products on host metabolism, *Mol. Cell*, **78**, 584-596, https://doi.org/10.1016/j.molcel.2020.03.005.
51. Molinaro, A., Bel Lassen, P., Henricsson, M., Wu, H., Adriouch, S., Belda, E., Chakaroun, R., Nielsen, T., Bergh, P. O., Rouault, C., André, S., Marquet, F., Andreelli, F., Salem, J. E., Assmann, K., Bastard, J. P., Forslund, S., Le Chatelier, E., Falony, G., Pons, N., Prifti, E., Quinquis, B., Roume, H., Vieira-Silva, S., Hansen, T. H., Pedersen, H. K., Lewinter, C., Sønderskov, N. B., Køber, L., Vestergaard, H., Hansen, T., Zucker, J. D., Galan, P., Dumas, M. E., Raes, J., Oppert, J. M., Letunic, I., Nielsen, J., Bork, P., Ehrlich, S. D., Stumvoll, M., Pedersen, O., Aron-Wisnewsky, J., Clément, K., and Bäckhed, F. (2020) Imidazole propionate is increased in diabetes and associated with dietary patterns and altered microbial ecology, *Nat. Commun.*, **11**, 5881, https://doi.org/10.1038/s41467-020-19589-w.
52. Koh, A., Molinaro, A., Ståhlman, M., Khan, M. T., Schmidt, C., Mannerås-Holm, L., Wu, H., Carreras, A., Jeong, H., Olofsson, L. E., Bergh, P. O., Gerdes, V., Hartstra, A., de Brauw, M., Perkins, R., Nieuwdorp, M., Bergström, G., and Bäckhed, F. (2018) Microbially produced imidazole propionate impairs insulin signaling through mTORC1, *Cell*, **175**, 947-961.e17, https://doi.org/10.1016/j.cell.2018.09.055.
53. Unden, G., Strecker, A., Kleefeld, A., and Kim, O. B. (2016) C_4-Dicarboxylate utilization in aerobic and anaerobic growth, *EcoSal Plus*, https://doi.org/10.1128/ecosalplus.ESP-0021-2015.
54. Van Hellemond, J. J., Klockiewicz, M., Gaasenbeek, C. P., Roos, M. H., and Tielens, A. G. (1995) Rhodoquinone and complex II of the electron transport chain in anaerobically functioning eukaryotes, *J. Biol. Chem.*, **270**, 31065-31070, https://doi.org/10.1074/jbc.270.52.31065.
55. Ramotar, K., Conly, J. M., Chubb, H., and Louie, T. J. (1984) Production of menaquinones by intestinal anaerobes, *J. Infect. Dis.*, **150**, 213-218, https://doi.org/10.1093/infdis/150.2.213.
56. Wargnies, M., Plazolles, N., Schenk, R., Villafraz, O., Dupuy, J. W., Biran, M., Bachmaier, S., Baudouin, H., Clayton, C., Boshart, M., and Bringaud, F. (2021) Metabolic selection of a homologous recombination-mediated gene loss protects *Trypanosoma brucei* from ROS production by glycosomal fumarate reductase, *J. Biol. Chem.*, **296**, 100548, https://doi.org/10.1016/j.jbc.2021.100548.
57. Sieburth, J. M. (1961) Antibiotic properties of acrylic acid, a factor in the gastrointestinal antibiosis of polar marine animals, *J. Bacteriol.*, **82**, 72-79, https://doi.org/10.1128/jb.82.1.72-79.1961.
58. Todd, J. D., Curson, A. R., Sullivan, M. J., Kirkwood, M., and Johnston, A. W. (2012) The *Ruegeria pomeroyi acuI* gene has a role in DMSP catabolism and resembles *yhdH* of *E. coli* and other bacteria in conferring resistance to acrylate, *PLoS One*, **7**, e35947, https://doi.org/10.1371/journal.pone.0035947.

59. Curson, A. R., Todd, J. D., Sullivan, M. J., and Johnston, A. W. (2011) Catabolism of dimethylsulphoniopropionate: microorganisms, enzymes and genes, *Nat. Rev. Microbiol.*, **9**, 849-859, https://doi.org/10.1038/nrmicro2653.
60. Raina, J. B., Tapiolas, D., Willis, B. L., and Bourne, D. G. (2009) Coral-associated bacteria and their role in the biogeochemical cycling of sulfur, *Appl. Environ. Microbiol.*, **75**, 3492-3501, https://doi.org/10.1128/AEM.02567-08.
61. Sogin, E. M., Michellod, D., Gruber-Vodicka, H. R., Bourceau, P., Geier, B., Meier, D. V., Seidel, M., Ahmerkamp, S., Schorn, S., 'D'Angelo, G., Procaccini, G., Dubilier, N., and Liebeke, M. (2022) Sugars dominate the seagrass rhizosphere, *Nat. Ecol. Evol.*, **6**, 866-877, https://doi.org/10.1038/s41559-022-01740-z.
62. Rameshkumar, N., and Nair, S. (2009) Isolation and molecular characterization of genetically diverse antagonistic, diazotrophic red-pigmented vibrios from different mangrove rhizospheres, *FEMS Microbiol. Ecol.*, **67**, 455-467, https://doi.org/10.1111/j.1574-6941.2008.00638.x.
63. Blum, M., Andreeva, A., Florentino, L. C., Chuguransky, S. R., Grego, T., Hobbs, E., Pinto, B. L., Orr, A., Paysan-Lafosse, T., Ponamareva, I., Salazar, G. A., Bordin, N., Bork, P., Bridge, A., Colwell, L., Gough, J., Haft, D. H., Letunic, I., Llinares-López, F., Marchler-Bauer, A., Meng-Papaxanthos, L., Mi, H., Natale, D. A., Orengo, C. A., Pandurangan, A. P., Piovesan, D., Rivoire, C., Sigrist, C. J. A., Thanki, N., Thibaud-Nissen, F., Thomas, P. D., Tosatto, S. C. E., Wu, C. H., and Bateman, A. (2025) InterPro: the protein sequence classification resource in 2025, *Nucleic Acids Res.*, **53**, D444-D456, https://doi.org/10.1093/nar/gkae1082.
64. Eberhardt, J., Santos-Martins, D., Tillack, A. F., and Forli, S. (2021) AutoDock Vina 1.2.0: New docking methods, expanded force field, and Python bindings, *J. Chem. Inf. Model.*, **61**, 3891-3898, https://doi.org/10.1021/acs.jcim.1c00203.